HHS Public Access

Author manuscript

J Thorac Cardiovasc Surg. Author manuscript; available in PMC 2020 August 21.

Published in final edited form as:

J Thorac Cardiovasc Surg. 2020 January ; 159(1): 88–97. doi:10.1016/j.jtcvs.2019.02.046.

A turbulence in-vitro assessment of ON-X and St. Jude Medical prostheses

Hoda Hatoum, PhD[a], **Pablo Maureira, MD, PhD**[b], **Lakshmi P. Dasi, PhD**[a]

[a]Department of Biomedical Engineering, The Ohio State University, Columbus, OH, USA

[b]Department of Cardiovascular Surgery, CHU de Nancy, Nancy, France

Abstract

Objective: The objective of this study is to investigate and compare the hemodynamic and turbulence characteristics upon implantation of St. Jude Medical (SJM) and ON-X bileaflet mechanical valves (BMHV). Both valves are considered highly successful BMHVs characterized by good clinical outcomes despite their numerous design differences. While thromboembolism remains the main disadvantage of BMHVs, ON-X has been shown to need less anti-coagulation therapy.

Methods: Hemodynamic assessment of a 23mm ON-X bileaflet mechanical valve and a 23mm bileaflet St. Jude Mechanical valve (SJM) implanted in an aortic root was performed under pulsatile physiological conditions. Time-resolved and phase-locked Particle-Image-Velocimetry images and high-speed imaging data were acquired. Pressure gradients (PG), effective orifice areas (EOA), dimensionless area index (AI), leaflet position tracking, velocity and Principal Reynolds shear stress (RSS) were calculated.

Results: (a) PG across ON-X was 4.15±0.099mmHg versus 4.75±0.048mmHg for SJM($p<0.001$). EOA across ON-X was 2.61±0.045cm^2 versus 2.36±0.022cm^2 for SJM($p<0.001$); (b) AI was higher with SJM (0.87±0.008) than with ON-X (0.73±0.013)($p<0.001$); (c)ON-X showed a fluctuating leaflet behavior during systole while SJM leaflets were stable; (d) at peak systole, the maximal velocity with ON-X was 1.86m/s versus 2.33m/s with SJM; (d) RSS was higher with ON-X compared with SJM at peak systole (95 versus 72Pa); (e) Higher velocity fluctuations was noted with ON-X.

Conclusions: This study shows that despite the design differences that characterize ON-X, the hemodynamic and turbulence parameters were not necessarily improved compared with SJM.

Address for correspondence and reprints: Lakshmi Prasad Dasi, PhD, Associate Professor, Department of Biomedical Engineering, The Ohio State University, 473 W 12th Ave., Columbus, OH 43210, TEL: (614) 247-8313, lakshmi.dasi@osumc.edu.

Conflict of Interest: Dr. Dasi reports having two patent applications on novel surgical and transcatheter valves. He also has a patent issued on vortex generators on heart valves and a patent application on super hydrophobic vortex generator enhanced mechanical heart valves. No other conflicts were reported.

Introduction

Bi-leaflet mechanical heart valves (BMHV) became the gold standard in mechanical heart valve implantation therapy. They are still widely used specifically in younger patients' populations in need of valve replacement. Throughout the past decades, mechanical valve designs have evolved in order to ameliorate valve hemodynamic and clinical performance, durability and reduce if not omit blood damage mainly platelet activation and blood hemolysis. However, blood trauma remains a seemingly non-preventable risk. Despite guideline-directed anti-coagulation therapy, thromboembolism has been the most common adverse effect associated with BMHV affecting around 0.1% to 5.7% per patient year (1). Anticoagulation therapy is associated with several risks such as hemorrhage (2–4). Clinical studies have shown that patients with BMHV have shortened platelet and red blood cell half-lives(5,6).

One of the most efficacious and popular bileaflet BMHV to date has been the St. Jude Mechanical valve (SJM) (St Jude Medical, Inc, St Paul, Minn) with over 35 years of proven clinical performance(7). SJM is characterized by an 85-degree leaflet-opening angle. Despite its low relative thrombogenicity, clinical studies with SJM mechanical valve have demonstrated a potential risk of valvular thrombosis that can lead to patient mortality (8–11). Another bileaflet mechanical valve, the ON-X (On-X Life Technologies, Inc (Austin, Tex)), emerged in 1996 and was FDA approved in 2001(12). In 2015, ON-X obtained an FDA approval that allows patients after 3 months from implantation to be managed at an international Normalized Ratio (INR) level of 1.5 to 2.0 that is closer to unmedicated INR(13). ON-X is characterized by a 90 degree leaflet opening angle in addition to a flared inlet orifice(12). Preliminary studies addressing the efficacy of ON-X demonstrated that the associated complications were comparable with other bileaflet BMHV in a similar population(12). ON-X valve demonstrated improved mean valve gradients and effective orifice areas compared with earlier bileaflet models(12,14). The most important observation found with ON-X was the decrease in thrombus formation that led to significantly reducing if not omitting the need for anti-coagulation therapy(15).

The assessment of blood damage in-vitro is usually performed through evaluating turbulent shear stresses, thus many attempts have been made to implement design modifications that reduce these stresses(16,17). Even though remarkable design developments in BMHVs over the last 50 years and new drug therapies have been established, the problems of platelet activation, hemolysis, and thromboembolism in BMHVs still persist.

The objective of this study is to investigate and compare the hemodynamic and turbulence characteristics upon implantation of SJM and ON-X BMHVs.

Methods

Valve selection and hemodynamic assessment

To evaluate post-valve hemodynamics and turbulence, measurements described below were conducted with a 23mm ON-X Life Technologies (ON-X) bileaflet mechanical valve (Aortic Heart Valve with Standard Sewing Ring (ONXA-23)) and a 23mm bileaflet St. Jude

Mechanical valve (SJM) (Masters Series mechanical heart valve PTFE cuff (23ATJ-503)) implanted in an aortic root. Valve dimensions are shown in Fig. 1a. Hemodynamic parameters were evaluated under pulsatile flow conditions created by a left heart simulator yielding physiological flow and pressure curves as previously described (18–25). The working fluid in this study was a blood-analogue mixture of water-glycerin (99% pure glycerine) producing a density of 1060Kg/m^3 and a kinematic viscosity of 3.5cSt. The cardiac output was set to be 5 L/min, the heart rate 60 beats per minutes and pressures of 120/80 mmHg. Three hundred consecutive cardiac cycles of aortic pressure, ventricular pressure and flow rate data were recorded at a sampling rate of 100Hz. The mean transvalvular pressure gradient (PG) is defined as the average of positive pressure difference between the ventricular and aortic pressure curves during forward flow.

The effective orifice area (EOA) is an important parameter to evaluate valve orifice opening. EOA was computed using the Gorlin's equation:

$$EOA = \frac{Q}{51.6\sqrt{PG}} \quad (1)$$

Where Q represents the root mean square aortic valve flow over the same averaging interval of the PG.

Because EOA is a function of the valve size, the area index (AI) is also calculated in equation (2) below. AI is an additional dimensionless characteristic that normalizes EOA by geometric valve size and shows a measure of the valve's resistance characteristics independent of the valve size.

$$AI = \frac{EOA}{A} \quad (2)$$

Where A represents the inner area in cm^2.

Particle Image Velocimetry (PIV)

For PIV, the flow was seeded with fluorescent PMMA-Rhodamine B particles with average diameters of 10 μm. For all cases, the velocity field within the distal flow region were measured using high spatial and temporal resolution PIV. Briefly, this involved illuminating the flow region using a laser sheet created by pulsed Nd;YLF single cavity diode pumped solid state laser coupled with external spherical and cylindrical lenses; while acquiring high-speed images of the fluorescent particles within the region. Time-resolved PIV images were acquired with a resulting spatial and temporal resolutions of 0.0296mm/pixel and 500Hz respectively. Phase locked measurements were recorded for 12 phases of the cardiac cycle starting from early systole (acceleration) and ending in mid-diastole repetitively 250 times with a spatial resolution of 0.0296mm/pixel. Refraction was corrected using a calibration in DaVis particle image velocimetry software (DaVis 7.2, LaVision Germany). Velocity vectors were calculated using adaptive cross-correlation algorithms. Further details of PIV measurements can be found in previous publications (18–26).

Vorticity Dynamics

Using the velocity measurements from PIV, vorticity dynamics were also evaluated distal to the valve. Vorticity is the curl of the velocity field and therefore captures rotational components of the blood flow shearing as well as visualizing turbulent eddies(25). Regions of high vorticity along the axis perpendicular to the plane indicate both shear and rotation of the fluid particles. Vorticity was computed using the following equation:

$$\omega_z = -\left(\frac{dV_x}{dy} - \frac{dV_y}{dx}\right) \quad (3)$$

Where ω_z is the vorticity component with units of s^{-1}; V_x and V_y are the x and y components of the velocity vector with units of m/s. The x and y directions are axial and lateral respectively with the z direction being out of measurement plane.

Reynolds shear stress (RSS)

Reynolds shear stress has been widely correlated to turbulence and platelet activation(27,28). It is a statistical quantity that measures the maximum (principal) Reynolds shear stress between fluid layers when fluid particles decelerate or accelerate while changing direction(29).

$$RSS = \rho\sqrt{\left(\frac{\overline{u'u'} - \overline{v'v'}}{2}\right)^2 + \left(\overline{u'v'}\right)^2} \quad (4)$$

Where ρ is the blood density and u' and v' are the instantaneous velocity fluctuations in the x and y directions respectively.

Statistics

All data are presented as mean ± standard deviation. Student's t test was used to compare the means and $p < 0.05$ was considered statistically significant. Probability density functions of the shear stress distribution were calculated and plotted. Analyses were performed over 300 replicates.

Results

Hemodynamic parameters

The pressure gradient (PG) across the ON-X valve was 4.15±0.099 mmHg and that across the bileaflet SJM valve was 4.75±0.048 mmHg ($p<0.001$). The effective orifice area (EOA) across the ON-X valve was 2.61±0.045 cm^2 and that across the SJM valve was2.36±0.022 cm^2 ($p <0.001$). The area index of the ON-X was calculated to be 0.73±0.013 versus a 0.87±0.008 for SJM ($p < 0.001$).

Leaflet tracking

Video 1 shows the opening and closing of the leaflets of every mechanical valve. Figure 1b shows the average instantaneous positions of the leaflet tip with respect to the mid-plane of each bileaflet valve (see figure inset) throughout the normalized opening phase. An

interesting feature that appear during the opening phase exclusively for the ON-X is the higher rate of leaflet fluctuations. However, the SJM valve shows a more stable behavior throughout systole.

Flow velocity fields

Flow velocity field is an important indicator of the flow velocity and vorticity state. While it is intuitive to assess the velocity, evaluating the vorticity that evaluates the local spinning of the fluid elements along with the characteristics of the shear layers (red and blue contours) do provide a comprehensive assessment of the flow post valve and help in the understanding of the resulting turbulence. The red and blue traces represent shear layers with red and blue being counterclockwise (CCW) and clockwise (CW) vorticity generated from the inner and outer surface boundary layers of each leaflet.

Figures 2 and 3 show the phase averaged velocity vectors and vorticity contours at different phases in the cardiac cycle for the 2 different valves. Video 2 shows the flow visualization across the valves. Qualitatively, as the valve opens, the shear layers start developing in both cases showing similar characteristics. Thinner shear layers are noted with the SJM compared to the ON-X along with a slower decay of the middle orifice ones until peak-systole is reached. More dissipation occurs with the ON-X in the peripheral jets compared with the SJM. Post peak systole, as shown in Figure 3, faster dissipation is again noted in the middle jet with the ON-X. During diastole, the flow structure topology is quite similar for both valves with more mixing clearly shown with the ON-X from the velocity vector direction. Quantitatively, at the beginning of the valve opening as shown in Figure 2, the flow field for both valves is characterized by a near zero velocity with the ON-X showing slightly higher velocity magnitude of 0.045±0.004 m/s compared with 0.008±0.001 m/s for SJM. Right before peak-systole, for the ON-X valve, the velocity reached 1.88±0.01 m/s in the middle jet and 1.94±0.02 m/s in the peripheral jets. For the SJM valve, the velocity reached 2.16±0.04 m/s in the middle jet and 2.21±0.01 m/s in the peripheral jets. During peak systole, and to better assess the variations of the velocity, Figure 4a shows the variation of the Vx profile at the horizontal centerline (Y=0) midway between the leaflets of the ON-X and the SJM valves during peak systole. The SJM exhibits higher velocities at the middle jet compared with the ON-X starting from 2.32m/s and ending at x = 30 mm with a velocity of 1.73 m/s (0.59 m/s difference). While for the ON-X, the velocity at the opening was shown to be 1.85 m/s and at x = 30 mm, 1.42m/s (0.43 m/s difference). In addition, during peak systole, Figure 4b shows the variation of Vx profile right at the tip of the leaflets post opening (at X=0) versus y during peak systole for the ON-X and the SJM valves. The velocity as shown in the previous point is higher with SJM compared with ON-X in the middle jet and the peripheral ones. In the middle jet at peak systole, the maximal velocity obtained with ON-X was calculated to be 1.86 m/s while 2.33 m/s for SJM. In the peripheral jets, the maximal velocity calculated with ON-X was shown to be 2.06±0.05 m/s and 2.42±0.07m/s for SJM. SJM peripheral jets nevertheless exhibit differences in maximal velocities. The difference between the middle jet velocity and the peripheral ones are close for both valve cases, despite having the ON-X more consistent as the peripheral jets velocity profiles are similar.

Reynolds shear stress (RSS) and velocity fluctuations field

Figures 5 and 6 display the distribution of Reynolds shear stress contours of the 2 valve cases at different time points throughout the cardiac cycle. Qualitatively during acceleration, the distribution of RSS looks different between both valves irrespective of the magnitude. More diffusion is noted with the ON-X during acceleration and prior to reaching mid-systole. At mid systole, higher level of irregular diffusion of momentum due to turbulent advection is noted with the ON-X in comparison with the SJM. More momentum diffusion continues to overwhelm the overall topology of the RSS contours in the ON-X compared to the SJM. This momentum diffusion is also obvious more notably in the peripheral jets of the SJM compared to the middle one. Decay in RSS is observed in both valves with increasing distance from the valve.

Quantitatively to better visualize the distribution of RSS throughout the flow region for both valves, probability density functions of RSS distribution were plotted and shown in Figures 7a, 7b and 7c during acceleration, peak systole and deceleration phases respectively. It is clear from the figures that peak systole is characterized by the highest magnitudes of RSS for both valves reaching around 95Pa in the ON-X case versus 72Pa for SJM. During acceleration, ON-X is characterized by higher likelihood to develop higher RSS up to 45Pa, however SJM is characterized by higher RSS magnitudes reaching around 58Pa. At peak systole, ON-X is characterized by higher likelihoods to develop higher RSS throughout. The same observation applies during deceleration with RSS magnitudes reaching 55Pa for ON-X and 42Pa for SJM. Velocity fluctuations characterize turbulent flows. A larger Vrms indicates a higher turbulence. Figure 7(d,e) shows the root mean square of the fluctuations in velocity (V_x') for the 2 different valves before, at and after mid-systole. Figure 7(f,g) shows the root mean square of the fluctuations in velocity (V_y') for the 2 different valves before, at and after mid-systole. It is obvious from Figure 8(a,b) that there is a more persisting level of fluctuations that occupies the downstream region post valve opening in x direction with the ON-X in comparison with the SJM.

Discussion

In this study, the differences engendered as a consequence of the 2 different bileaflet BMHV ON-X and SJM were evaluated via: (1) hemodynamic parameters in terms of pressure gradients, effective orifice areas and area index; and (2) flow visualization in terms of turbulence parameters. The importance of studying turbulence stems from its effect on blood damage particularly platelet activation, hemolysis, and effects on pressure recovery and drop.

Effect of valve design on hemodynamic parameters

The pressure gradient data among the 2 BMHV were insignificantly different. Clinical studies have shown that for ON-X valves whose sizes range from 19 to 25 mm, the expected pressure gradients fall within 4.7 to 8.3mmHg, and effective orifice areas within 1.5 to 2.7 cm^2 as per Palatianos et al(14). Similarly, the pressure gradient obtained with the SJM valve falls within the clinical range (average 6.9mmHg) obtained by Izzat et al(30). Another study by Butany et al(31) showed that the average PGs obtained with an SJM range from 3.0

to5.2mmHg. The values obtained in this in-vitro study fall within the range of those obtained in vivo.

Xu et al showed in a population study that regardless of the size of the valve and the diversity of the patients, the ON-X yielded equal or higher EOAs. From a design perspective, the ON-X valve is characterized by a larger internal diameter (21.4mm) compared with the same tissue annulus diameter and valve size SJM (18.6mm) (Fig. 1a). These additional mms seem to be advantageous for the ON-X and seem to explain the higher EOAs obtained in-vivo and in-vitro. Nevertheless, non-dimensional area index that normalizes EOA to the internal diameter of the valve indicates how well a valve design utilizes its total internal geometric orifice area. Thus, it provides a measure of the valve's resistance characteristics independent of the size higher performance with SJM compared to ON-X.

Additionally, from a physical perspective, flows from reservoirs to smaller orifices with sharp edges are accompanied by high entry losses. These entry losses can be mitigated or decreased by having a rounded edge entry orifice(32), as is the case with the ON-X design. The flared inlet design of the ON-X valve as opposed to the SJM bileaflet mechanical valve, allows the flow to remain attached to the boundary without any separation thus with minimal losses. This design and fluid mechanism may also be partially responsible for the lower pressure gradients and higher EOAs obtained with the ON-X.

Effect of leaflet and valve design on hemodynamic behavior

As highlighted in the results, the ON-X leaflets show a higher degree of leaflet fluctuation compared with the SJM bileaflet valve. The relatively constant and consistent leaflet motion of the SJM during systole emphasizes one aspect of the valve design that is the smaller and shorter leaflet design of the SJM. The larger the leaflets the harder it is to maintain a stable behavior under the flow conditions. In addition to that, the incomplete leaflet opening of the SJM leaflets allows the fluid pressure force to keep the leaflet pressed open against the hinge. While in the ON-X case, and due to the complete opening of the leaflets, this force is not present leading to a free oscillation of the leaflet. That is also clear at the beginning of valve opening in Figure 1b where the ON-X responds faster (sharp slope) to the flow condition while the SJM opening phase is slower at the beginning (constant and slowly decreasing leaflet tracking curve). The effect of leaflet fluctuations will be further discussed in details in the coming sections.

Flow velocity fields and profiles and relationship with turbulence

RSS and flow velocity fields help identify the spatio-temporal locations of flow instabilities and quantify overall turbulence characteristics(33). They can also provide an additional assessment of valve performance(25). Previous in-vitro studies investigated the risk of blood damage and attempted to set thresholds that signal the beginning of platelet activation. However, so far thresholds are not well-established, and the characterization of turbulent stress is still disputable. Hung et al. reported platelet damage at 100–165 dynes/cm^2 with an exposure time of 102 s(34). Williams et al established the onset of platelet activation at 130 dynes/cm^2 under an exposure time of 1023 s(35). Ramstack et al. reported platelet activation

at 300–1000 dynes/cm^2 at an exposure time of 10s(36). A study by Kameneva et al showed that turbulent flow increases hemolysis risk compared with laminar flow(37) given the same exposure time. Another study by Quinlan et al (38) explains that in turbulent flow through a prosthetic heart valve, the flow-induced stress on a blood cell is estimated to be at least an order of magnitude less than the Reynolds stress(38). Antiga and Steinman (39) highlighted the importance of cell-to-cell interaction in blood damage with turbulent flow. They also explain how turbulent velocity fluctuations can give rise to viscous shear stress however they acknowledge that RSS is a potential indicator of blood damage.

The jet through ON-X is characterized by lower velocities compared with SJM, and this is expected due to the larger orifice that allows blood to flow. Faster vorticity dissipation was observed with the ON-X in addition to higher levels of velocity fluctuations in the x and y directions. These fluctuations were evident in Video 1 and Figure 1b where the leaflet was “oscillating” throughout the valve opening phase. The fluctuations in the y-direction are tightly related to the unsteadiness explained in the stream-wise component of velocity, and vorticity fields above showing a more stable behavior for SJM. The distribution of the principal RSS of both showed great differences in terms of magnitudes and of likelihoods to develop high RSS. These results are also confirmed by those in Figures 7(a,b) and 7(c,d) where more fluctuations in the x and y directions are observed with ON-X compared with SJM.

Hemodynamics and in-vivo anti-coagulant results

Several clinical studies have been conducted using the ON-X mechanical valve and demonstrated promising results shortly after implantation and on the long run, particularly when it comes to the absence of thrombus formation with no or minimal anticoagulation therapy(12,15). While ON-X is characterized by lower velocities and higher effective orifice areas, turbulence results have shown quite important parameters that do not constitute a decisive indication or proof for a decision of whether omitting or reducing anti-coagulant therapy. Hinges flow dynamics of both BMHV were not investigated in this study. Previous studies have shown that a proper bileaflet valve function necessitates proper flow fields within hinge mechanisms(40,41). Within these hinge mechanisms, stagnation regions can form which trigger the formation and development of thrombus(7). Investigating the flow in the hinges does not fall within the scope of this work, however future studies will be performed.

Limitations

Several limitations are present in this study. The blood-analog fluid used is of constant viscosity while blood is a non-Newtonian fluid. The change in viscosity does not affect the pressure or pressure gradient measurement, but certainly it does affect the leaflet kinematics, the overall flow structures onset and formation and blood damage (42–44). To precisely evaluate these differences, further experiments are needed. In addition, 2D PIV is used in this study and only size 23mm is tested.

Conclusion

The turbulence and hemodynamic performances of 2 BMHVs ON-X and SJM were assessed in this study. Figure 8 provides a summary of the study. ON-X showed slightly smaller PGs and higher EOAs compared with SJM. The dimensionless area index was higher with SJM. The flow velocity fields and RSS contours were different between the valves with higher velocities and vorticities with SJM whereas higher fluctuating velocities in the x and y directions and RSS with ON-X. This study shows that despite the design differences between the 2 valves, hemodynamic and turbulence parameters are close. Further studies are required to investigate the flow in the hinges along with the effect of each of these valves on blood cells in order to understand and relate more thoroughly hemodynamics to blood trauma.

Supplementary Material

Refer to Web version on PubMed Central for supplementary material.

Funding:

The research done was partly supported by National Institutes of Health (NIH) under Award Number R01HL119824 and R01HL135505.

Abbreviations, symbols and terminology

SJM	St. Jude Medical
PG	Pressure Gradient
RSS	Reynolds shear stress
PIV	Particle Image Velocimetry
EOA	Effective Orifice Area
AI	Area Index
BMHV	Bi-leaflet Mechanical Heart Valve

References

1. Murphy DW, Dasi LP, Vukasinovic J, Glezer A, Yoganathan AP. Reduction of procoagulant potential of b-datum leakage jet flow in bileaflet mechanical heart valves via application of vortex generator arrays. Journal of biomechanical engineering 2010; 132:071011. [PubMed: 20590289]
2. Poller L, Jacobson A, Deykin D et al. Managing oral anticoagulant therapy. Chest 2001;119:22S–38S. [PubMed: 11157641]
3. Cannegieter SC, Rosendaal F, Wintzen A, Van der Meer F, Vandenbroucke J, Briet E. Optimal oral anticoagulant therapy in patients with mechanical heart valves. New England Journal of Medicine 1995;333:11–17. [PubMed: 7776988]
4. Vandenmeer F, Rosendaal F, Vandenbroucke J, Briet E. Bleeding complications in patients treated with oral anticoagulants in a routine situation. Thrombosis and Haemostasis: FK SCHATTAUER VERLAG GMBH PO BOX 10 45 45, LENZHALDE 3, D-70040 STUTTGART, GERMANY, 1993:982–982.

5. Dale J, Myhre E. Intravascular hemolysis in the late course of aortic valve replacement. Relation to valve type, size, and function. American heart journal 1978;96:24–30. [PubMed: 655106]
6. Harker LA, Slichter SJ. Studies of platelet and fibrinogen kinetics in patients with prosthetic heart valves. New England Journal of Medicine 1970;283:1302–1305. [PubMed: 5478451]
7. Saxena R, Lemmon J, Ellis J, Yoganathan A. An in vitro assessment by means of laser Doppler velocimetry of the medtronic advantage bileaflet mechanical heart valve hinge flow. The Journal of thoracic and cardiovascular surgery 2003;126:90–98. [PubMed: 12878943]
8. Baudet EM, Oca C, Roques X et al. A 5 1/2 year experience with the St. Jude Medical cardiac valve prosthesis. Early and late results of 737 valve replacements in 671 patients. The Journal of thoracic and cardiovascular surgery 1985;90:137–144. [PubMed: 3874324]
9. Chang B, Lim S, Kim D et al. Long-term results with St. Jude Medical and CarboMedics prosthetic heart valves. The Journal of heart valve disease 2001;10:185–194; discussion195. [PubMed: 11297205]
10. Ibrahim M, O'Kane H, Cleland J, Gladstone D, Sarsam M, Patterson C. The St. Jude Medical prosthesis: a thirteen-year experience. The Journal of thoracic and cardiovascular surgery 1994;108:221–230. [PubMed: 8041170]
11. Masters R, Pipe A, Walley V, Keon W. Comparative results with the St. Jude Medical and Medtronic Hall mechanical valves. The Journal of thoracic and cardiovascular surgery 1995;110:663–671. [PubMed: 7564432]
12. Chaudhary R, Garg J, Krishnamoorthy P et al. On-X valve: the next generation aortic valve. Cardiology in review 2017;25:77–83. [PubMed: 28170357]
13. Jackson L, Yenney I. FDA Approval: On-X aortic valves with less warfarin. 2015.
14. Palatianos GM, Laczkovics AM, Simon P et al. Multicentered European study on safety and effectiveness of the On-X prosthetic heart valve: intermediate follow-up. The Annals of thoracic surgery 2007;83:40–46. [PubMed: 17184628]
15. Williams MA. The On-X heart valve: mid-term results in a poorly anticoagulated population. The Journal of heart valve disease 2006;15:80–86. [PubMed: 16480016]
16. Vongpatanasin W, Hillis LD, Lange RA. Prosthetic heart valves. New England Journal of Medicine 1996;335:407–416. [PubMed: 8676934]
17. Dasi LP, Simon HA, Sucosky P, Yoganathan AP. Fluid mechanics of artificial heart valves. Clinical and experimental pharmacology and physiology 2009;36:225–237. [PubMed: 19220329]
18. Hatoum H, Dasi L. Sinus Hemodynamics in Representative Stenotic Native Bicuspid and Tricuspid Aortic Valves: An In-Vitro Study. Fluids 2018;3:56.
19. Hatoum H, Dollery J, Lilly SM, Crestanello J, Dasi LP. Impact of patient-specific morphologies on sinus flow stasis in transcatheter aortic valve replacement: An in vitro study. The Journal of thoracic and cardiovascular surgery 2018.
20. Hatoum H, Dollery J, Lilly SM, Crestanello JA, Dasi LP. Implantation Depth and Rotational Orientation Effect on Valve-in-Valve Hemodynamics and Sinus Flow. The Annals of thoracic surgery 2018.
21. Hatoum H, Dollery J, Lilly SM, Crestanello JA, Dasi LP. Sinus Hemodynamics Variation with Tilted Transcatheter Aortic Valve Deployments. Annals of biomedical engineering 2018:1–10.
22. Hatoum H, Dollery J, Lilly SM, Crestanello JA, Dasi LP. Effect of severe bioprosthetic valve tissue ingrowth and inflow calcification on valve-in-valve performance. Journal of biomechanics 2018;74:171–179. [PubMed: 29753455]
23. Hatoum H, Heim F, Dasi LP. Stented valve dynamic behavior induced by polyester fiber leaflet material in transcatheter aortic valve devices. Journal of the mechanical behavior of biomedical materials 2018;86:232–239. [PubMed: 29986298]
24. Hatoum H, Moore BL, Maureira P, Dollery J, Crestanello JA, Dasi LP. Aortic sinus flow stasis likely in valve-in-valve transcatheter aortic valve implantation. The Journal of thoracic and cardiovascular surgery 2017;154:32–43. e1. [PubMed: 28433356]
25. Hatoum H, Yousefi A, Lilly S, Maureira P, Crestanello J, Dasi LP. An in vitro evaluation of turbulence after transcatheter aortic valve implantation. The Journal of thoracic and cardiovascular surgery 2018.

26. Hatoum H, Moore BL, Dasi LP. On the significance of systolic flow waveform on aortic valve energy loss. Annals of biomedical engineering 2018:1–10.
27. Giersiepen M, Wurzinger L, Opitz R, Reul H. Estimation of shear stress-related blood damage in heart valve prostheses--in vitro comparison of 25 aortic valves. The International journal of artificial organs 1990;13:300–306. [PubMed: 2365485]
28. Nygaard H, Giersiepen M, Hasenkam J et al. Two-dimensional color-mapping of turbulent shear stress distribution downstream of two aortic bioprosthetic valves in vitro. Journal of biomechanics 1992;25:437–440.
29. Gunning PS, Saikrishnan N, McNamara LM, Yoganathan AP. An in vitro evaluation of the impact of eccentric deployment on transcatheter aortic valve hemodynamics. Annals of biomedical engineering 2014;42:1195–1206. [PubMed: 24719050]
30. Izzat MB, Birdi I, Wilde P, Bryan AJ, Angelini GD. Comparison of hemodynamic performances of St. Jude Medical and CarboMedics 21 mm aortic prostheses by means of dobutamine stress echocardiography. The Journal of thoracic and cardiovascular surgery 1996;111:408–415. [PubMed: 8583814]
31. Butany J, Ahluwalia MS, Munroe C et al. Mechanical heart valve prostheses: identification and evaluation. Cardiovascular Pathology 2003;12:1–22. [PubMed: 12598013]
32. White FM. Fluid mechanics, in SI units. McGraw-Hill, 2011.
33. Hatoum H, Dasi LP. Reduction of Pressure Gradient and Turbulence Using Vortex Generators in Prosthetic Heart Valves. Annals of biomedical engineering 2018:1–12.
34. Hung T, Hochmuth R, Joist J, Sutera S. Shear-induced aggregation and lysis of platelets. ASAIO Journal 1976;22:285–290.
35. Williams A. Release of serotonin from human platelets by acoustic microstreaming. The Journal of the Acoustical Society of America 1974;56:1640–1643. [PubMed: 4427036]
36. Ramstack J, Zuckerman L, Mockros L. Shear-induced activation of platelets. Journal of biomechanics 1979;12:113–125. [PubMed: 422576]
37. Kameneva MV, Burgreen GW, Kono K, Repko B, Antaki JF, Umezu M. Effects of turbulent stresses upon mechanical hemolysis: experimental and computational analysis. ASAIO journal 2004;50:418–423. [PubMed: 15497379]
38. Quinlan NJ, Dooley PN. Models of flow-induced loading on blood cells in laminar and turbulent flow, with application to cardiovascular device flow. Annals of biomedical engineering 2007;35:1347–1356. [PubMed: 17458700]
39. Antiga L, Steinman DA. Rethinking turbulence in blood. Biorheology 2009;46:77–81. [PubMed: 19458411]
40. Gross J, Shu M, Dai F, Ellis J, Yoganathan A. A microstructural flow analysis within a bileaflet mechanical heart valve hinge. The Journal of heart valve disease 1996;5:581–590. [PubMed: 8953435]
41. Leo H-L, He Z, Ellis JT, Yoganathan AP. Microflow fields in the hinge region of the CarboMedics bileaflet mechanical heart valve design. The Journal of thoracic and cardiovascular surgery 2002;124:561–574. [PubMed: 12202873]
42. Moore B, Dasi LP. Spatiotemporal complexity of the aortic sinus vortex. Experiments in fluids 2014;55:1770. [PubMed: 25067881]
43. De Vita F, De Tullio M, Verzicco R. Numerical simulation of the non-Newtonian blood flow through a mechanical aortic valve. Theoretical and computational fluid dynamics 2016;30:129–138.
44. Pohl M, Wendt MO, Werner S, Koch B, Lerche D. In vitro testing of artificial heart valves: comparison between Newtonian and non-Newtonian fluids. Artificial organs 1996;20:37–46. [PubMed: 8645128]

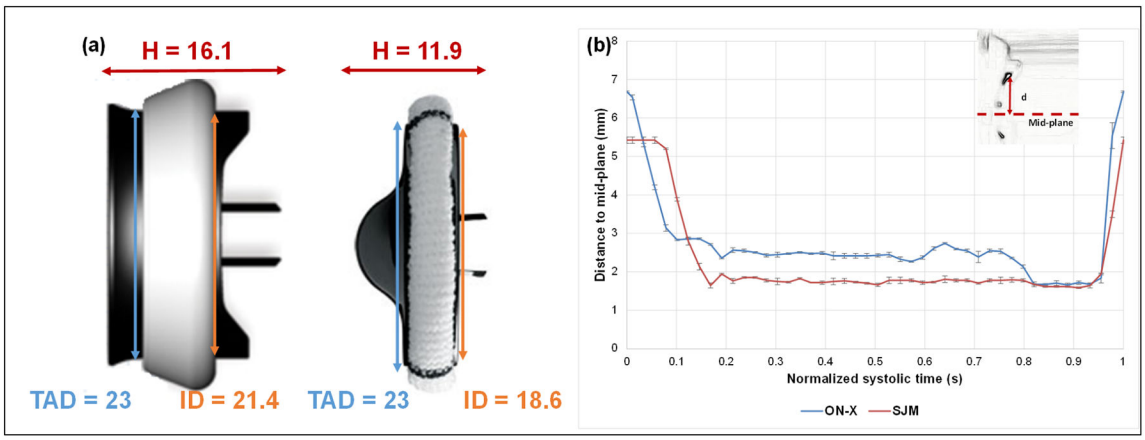

Figure 1:

(a) Geometric dimensions of the 2 valves: ON-X on the left and SJM on the right; TAD denotes tissue annulus diameter, H denotes height and ID denotes internal diameter; (b) Average Instantaneous positions of the leaflet tip with respect to the mid-plane of the valve throughout the normalized opening phase. Error bars are ± standard deviation. Larger internal orifice and profile are measured with ON-X. More leaflet fluctuations are observed with ON-X.

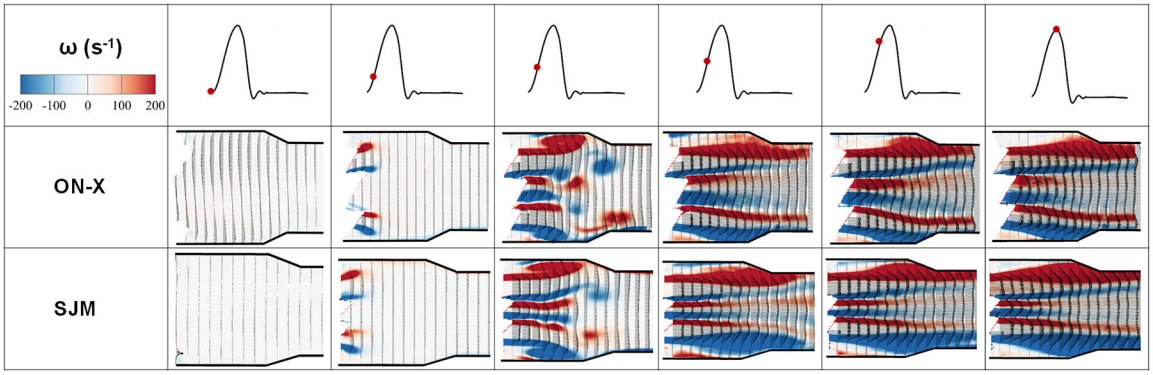

Figure 2:

Phase averaged velocity vectors and vorticity contours at different phases in the cardiac cycle (until peak systole) for the 2 different valves. Different flow structures are dictated by the different flow behaviors in the presence of the 2 different valves.

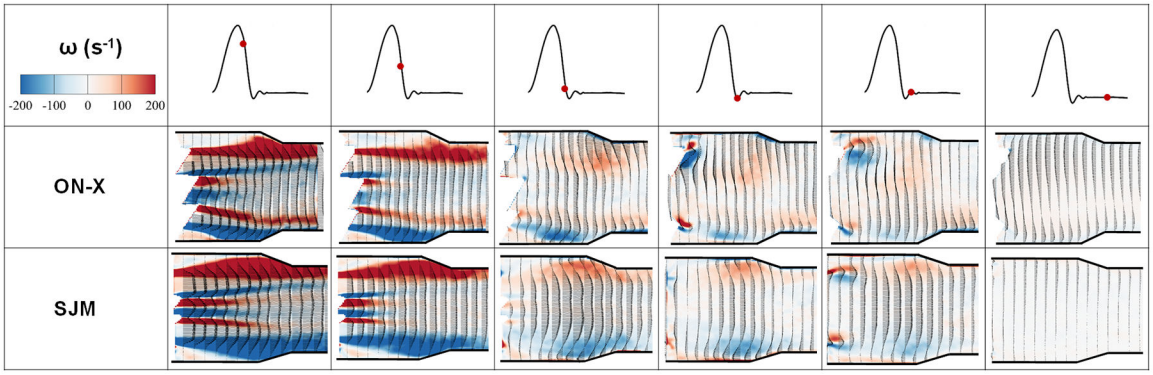

Figure 3:
Phase averaged velocity vectors and vorticity contours at different phases in the cardiac cycle (post peak systole) for the 2 different valves. Different flow structures are dictated by the different flow behaviors in the presence of the 2 different valves.

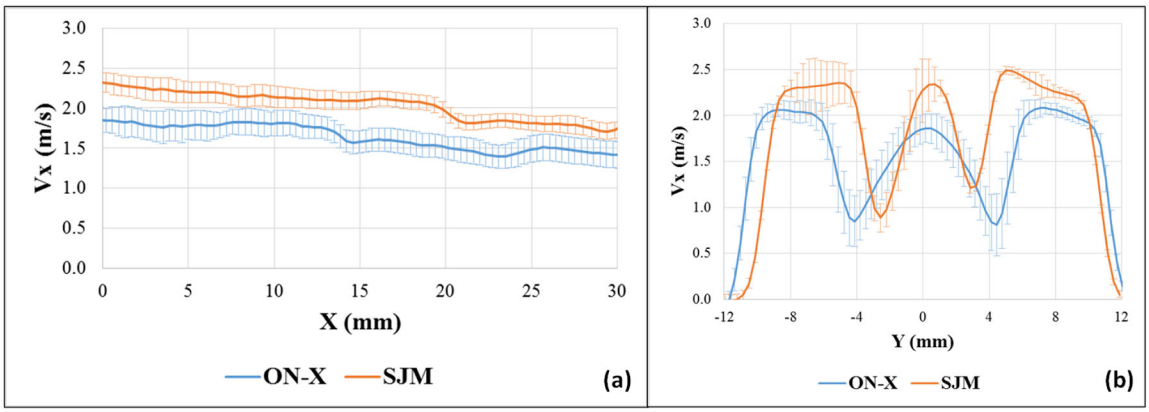

Figure 4:

(a) V_x profile at the horizontal centerline (Y=0) midway between the leaflets of the ON-X and the SJM valves during peak systole and (b) V_x profile right at the tip of the leaflets post opening (X=0) versus y during peak systole for the ON-X and the SJM valves. Error bars are ± standard deviation. Vx is the streamwise component of velocity. Higher velocities are obtained with SJM compared to ON-X.

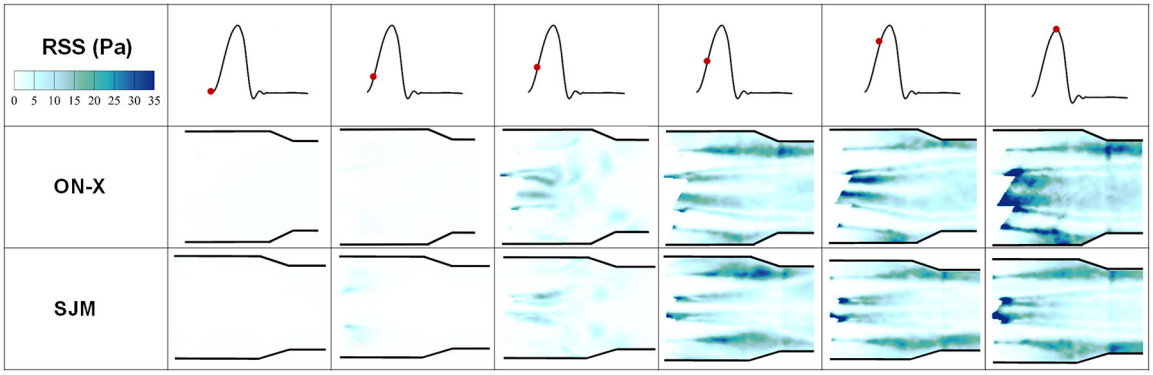

Figure 5:
Principal Reynolds shear stress (RSS) contours of the 2 valve cases at different time points throughout the cardiac cycle. Higher RSS magnitudes are obtained with ON-X compared to SJM.

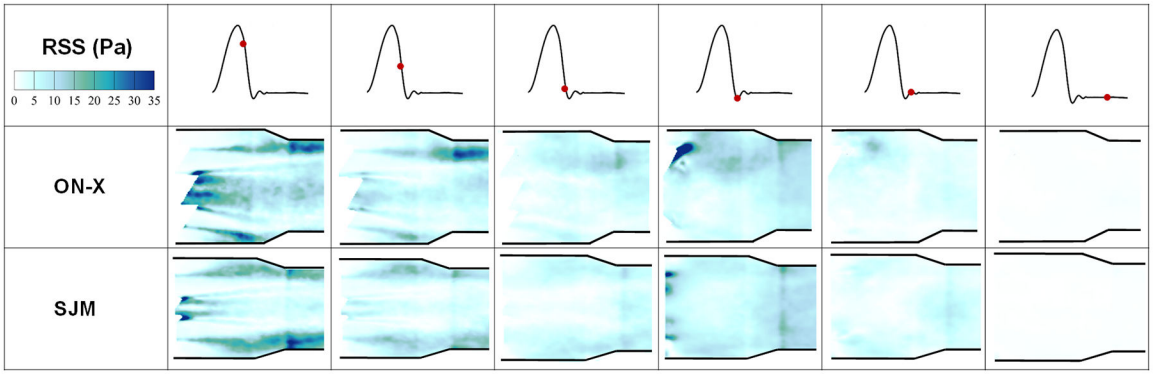

Figure 6:
Principal Reynolds shear stress (RSS) contours of the 2 valve cases at different time points throughout the cardiac cycle. Higher RSS magnitudes are obtained with ON-X compared to SJM.

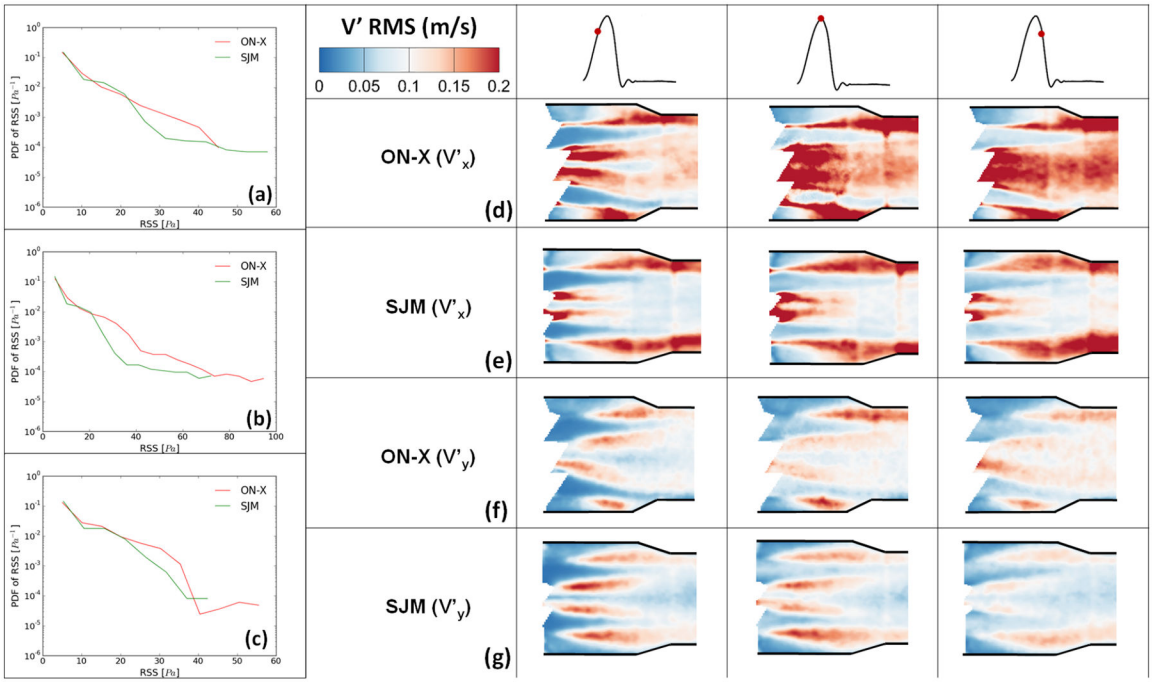

Figure 7:

Root mean square of the fluctuations in velocity (a,b) V_x' and (c,d) V_y' for the 2 different valves before, at and after mid-systole. Reynolds Shear Stress (RSS) and velocity fluctuations span a wider range with ON-X compared with SJM.

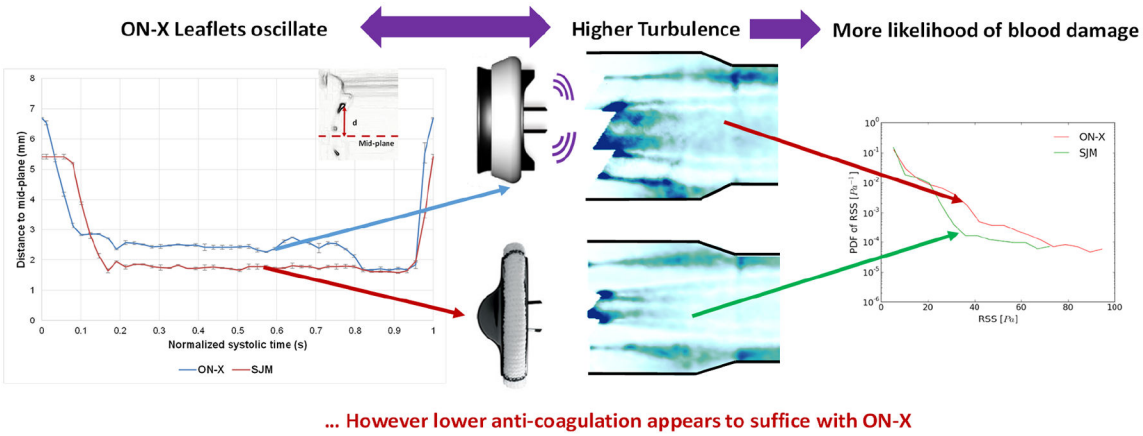

Figure 8:

ON-X shows more turbulent fluctuation than SJM yet lower anti-coagulation seems to suffice.